

MODELING HYSTERESIS OBSERVED
IN THE HUMAN ERYTHROCYTE
VOLTAGE-DEPENDENT CATION CHANNEL

HENRIK FLYVBJERG

Department of Micro and Nanotechnology, Technical University of Denmark
Konges Lyngby, Denmark

EWA GUDOWSKA-NOWAK

The Marian Smoluchowski Institute of Physics
and
M. Kac Complex Systems Research Center, Jagiellonian University
Reymonta 4, 30-059 Kraków, Poland
gudowska@th.if.uj.edu.pl

PALLE CHRISTOPHERSEN

NeuroSearch, Pederstrupvej 93, 2750 Ballerup, Denmark

POUL BENNEKOU

August Krogh Institute, Universitetsparken 13, 2100, Copenhagen, Denmark

(Received November 22, 2012; revised version received December 3, 2012)

The non-selective voltage-activated cation channel from human red cells, which is activated at depolarizing potentials, has been shown to exhibit counter-clockwise gating hysteresis. Here, we analyze this phenomenon with the simplest possible phenomenological models. Specifically, the hysteresis cycle, including its direction, is reproduced by a model with 2×2 discrete states: the normal open/closed states and two different states of “gate tension”. Rates of transitions between the two branches of the hysteresis curve are modeled with single-barrier kinetics by introducing a real-valued “reaction coordinate” parametrizing the protein’s conformational change between the two states of gate tension. The resulting scenario suggests a reanalysis of former experiments with NSVDC channels.

DOI:10.5506/APhysPolB.43.2117

PACS numbers: 87.16.Uv, 87.15.He, 87.16.Dg

1. Introduction

Ion channels are membrane proteins capable of mediating a gated, selective, and electrogenic transport of ions across the cell membrane. They are found in all mammalian cells and their physiological roles range from bulk ion transport to subtle electrogenic signaling. Many ion channels are closed most of the time, but open in response to specific physiological stimuli, such as altered concentration of specific compounds, membrane potential changes, or temperature shifts. As the activating stimulus disappears, the ion channel is usually deactivated [1]. However, even with maintained stimulus many ion channels close down — a phenomenon known as inactivation or desensitization [1]. Explicit references to memory-effects in ion channel gating are rare in the literature, but hysteretic gating behavior has been described for a channel forming peptide, alamethicin [2] as well as native mammalian channels, such as ligand-gated (NMDA-receptor) [3] and voltage-gated channels (HERG-like channel [4, 5] and red cell voltage-dependent cation channels [6–8]). Recently, a member of the TRP family of cation channels (TRPV3) has been shown to exhibit clear temperature hysteresis, possibly adding polarity of temperature changes as a sensory modality for dorsal root ganglion neurons [9]. Hysteresis may, however, well be a normal kinetic behavior with potentially important physiological implications, and although none of the described hysteresis phenomena are yet understood at the molecular level, phenomenological models can be established, as shown in the following sections.

In magnetic materials, hysteresis is a common phenomenon, and well understood theoretically. This may seem of little relevance for ion channels, because magnetic behavior is a collective phenomenon that occurs only when an effectively infinite number of atomic magnetic dipoles interact. In contrast, ion channel hysteresis must be explained with just the few degrees of freedom of the fully folded protein that forms the individual channel. It is, however, only the multiple ground states caused by magnetism that is needed to have hysteresis. Consequently, one can understand ion channel hysteresis through a close analogy with magnetic hysteresis: The ion channel protein corresponds to a chunk of magnetic material described by the Ising model [10], which is the simplest possible model of magnetism. The gate corresponds to one particular atomic dipole in this chunk. Gate and dipole both can take only two values, ± 1 . Which one is favored depends on which of its two magnetic states the chunk is in, and on the value of an external magnetic field that interacts only with the particular dipole that corresponds to the gate. Similarly, the open-probability of the gate depends on which one of two postulated conformational states the protein is in, and on the value of the membrane potential interacting only with the gate. It is then sufficient to invoke Newton's third law to demonstrate hysteresis in both systems.

The presentation below does not rely on this analogy with magnetism, however. Instead, we explain our modeling from basic principles. We present two closely related minimal models, referred to as 2×2 and $2 \times \mathcal{R}$. The 2×2 -model has the two states of the gate (open/closed) as well as the two other conformational states of the protein, two states of different “gate tension.” The $2 \times \mathcal{R}$ -model is an extension of the 2×2 -model in which the two states of different gate tension have been replaced with a real-valued reaction coordinate for conformational change in order to describe thermally activated barrier crossing. These models provide a formal biophysical description of gating hysteresis. They also suggest a mechanism responsible for the hysteresis, as we have seen: a secondary conformational change in part of the ion channel, apart from the gating, but functionally linked to it. The description below is so general, however, that any other mechanism which causes a similar bias in the gate’s open-probability, is described by it as well.

2. Experimental basis

The data used for the analysis were obtained from an inside-out excised patch from a human red blood cell bathed symmetrically in 300 mM KCl. A plot of some of these data was published in [8]. From a holding potential of -15 mV (close to normal red cell potential), the command potential was increased in 10 mV steps of 3 min duration till $+100$ mV was reached, then decreased in steps that back-tracked the positive steps. After 15 minutes at the original holding potential, the command sequence was repeated once more. The open-state probabilities were calculated from the series of 3 min. recordings. Although close inspection revealed that the channel exhibited multiple conductance states, see Fig. 1, a dominating state of 33 pS was observed with more than 95% probability, and no changes in the distribution of the open states as function of voltage was observed. As illustrated in Figs. 2 and 3, the open-state probability at a given voltage depends on the system’s history with regard to the holding potential, the channel being far more active at a given command voltage after a previous activation at $+100$ mV or more. Since the occurrence of the individual conductance states seemed to be independent of the command potential as well as the prehistory, it was decided to use a simple 2-state description for the modeling. The open-state probability p_o was consequently calculated as $p_o = 1 - p_{cl}$, where p_{cl} is the closed-state probability.

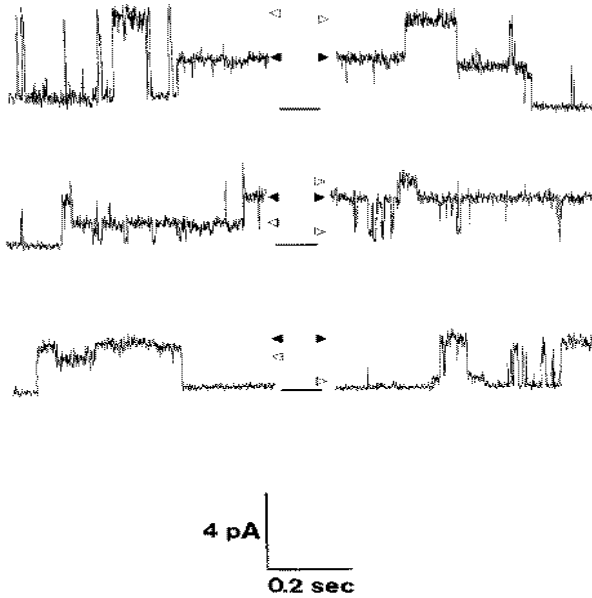


Fig. 1. Multiple conductance states: The traces were recorded at a command potential of +100 mV, and show the multiple conductance levels of the NSVDC channel. Black triangles indicate a dominating single level with a conductance of 33 pS. The traces shown were selected for their high occurrence of multiple states. In 95% of the time that the gate is open, only the 33 pS-state occurs.

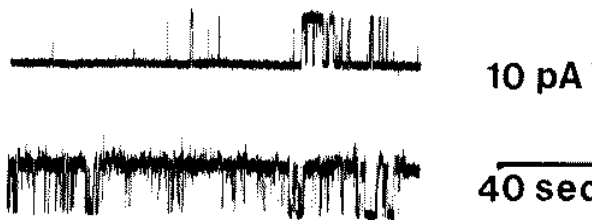


Fig. 2. Configurational changes of ion channel reflected in the pattern it opens and closes with as function of history. The traces shown were recorded from the red cell non-selective voltage activated cation (NSVDC) channel, clamped at +70 mV. When the command potential was increased step-wise from negative to positive values, the upper trace was obtained at +70 mV. When the command potential was decreased again, after full activation at +100 mV, the lower trace was obtained. Due to the heavy filtering (cut-off frequency 1 Hz) fast events are underrepresented.

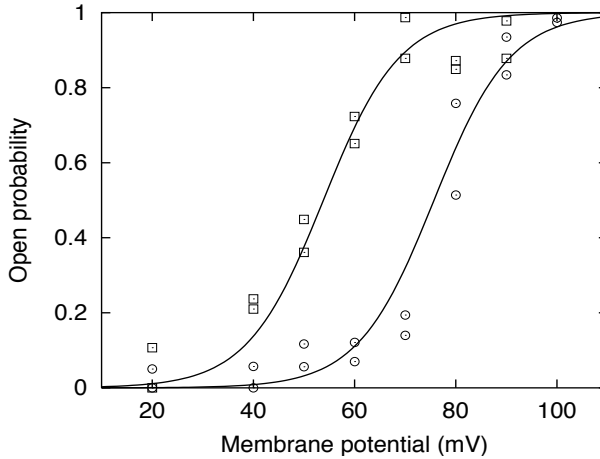


Fig. 3. The open state probability p_o as a function of the membrane potential V for V increasing from -15 mV (circles) and for V decreasing from $+100$ mV (squares). The two curves are the result of a least-squares fit of p_o in Eq. (7) to the data for increasing and decreasing membrane potential. The same value for α was used for both branches of the hysteresis cycle, with two different values for V_b . The sum of the χ^2 -values for the two branches was minimized w.r.t. V_+ (upper branch), V_- (lower branch), and α , resulting in $V_+ = 54$ mV, $V_- = 76$ mV, and $\alpha = 0.13$ mV $^{-1}$ (in units of $k_B T$), which corresponds to a gating charge $z = 3.4$ according to Eq. (9). The latter value is reasonable, given our moderate precision, as gating charges range from approxim. 4 for K^+ channels to 6–7 for Na^+ channels [1].

3. Simplest possible model: 2×2

We want to model the experimental data shown in Fig. 3 with as simple a model as possible. So the issue is: what is the simplest model that can describe hysteresis in a voltage-activated ion channel's probability of being open, p_o , under changes in membrane potential V ?

3.1. The two branches of the hysteresis cycle

Even before ion channels were discovered, Hodgkin and Huxley suggested the mechanism of voltage-gated ion channels, and that Boltzmann statistics describes their probability of being open or closed, including the voltage-dependence of this probability [11, p. 503]. Now an established fact [1, p. 55], we use this mechanism to describe the two branches of the hysteresis cycle independently of each other in the present subsection. This amounts to a repetition of well-known equations, but establishes the take-off point for the following subsection's modeling of hysteresis.

We concern ourselves with only two states of the gate, open and closed. We parametrize these two states with a binary variable $\sigma_g = \pm 1$, $+1$ denoting open, -1 denoting closed. We associate an internal energy $E(\sigma_g)$ with each of the two states, and assume that Boltzmann statistics describes the probability for a channel to be open or closed, with transitions between the two states being thermally activated barrier crossings in an energy landscape that we do not detail here. Then the probability that a channel is open or closed is

$$p(\sigma_g) = \frac{e^{-E(\sigma_g)}}{e^{-E(+1)} + e^{-E(-1)}} = \frac{1}{1 + e^{\sigma_g \Delta E}}, \quad (1)$$

where the internal energy is given in units of $k_B T$ and

$$\Delta E = E(+1) - E(-1). \quad (2)$$

In particular,

$$p_o = p(+1) = \frac{1}{1 + e^{\Delta E}} \quad (3)$$

which can be equated to the experimentally observable

$$p_o = \frac{\bar{t}_o}{\bar{t}_o + \bar{t}_{cl}}, \quad (4)$$

where \bar{t}_o and \bar{t}_{cl} are the mean durations of the open and closed states of the gate.

The sigmoid character of the experimental data's two branches in Fig. 3 begs the physical interpretation suggested by Hodgkin and Huxley: there is a gating charge ze , and the difference in internal energy between the open and closed states, ΔE consists of two terms $(w + zeV)/k_B T$, a mechanical energy difference w , as if the gate were pulling against a spring when opening, and an electrical energy difference proportional to the membrane potential V , with positive values favoring opening. Thus, we can write

$$\Delta E = -\alpha(V - V_b), \quad (5)$$

where α is a positive constant of proportionality, V_b is the membrane potential at which the open and closed states have the same internal energy, hence are equally probable, and $b = \pm$ is a subscript that distinguishes which branch of the hysteresis cycle we refer to, with $+$ denoting the upper branch and $-$ denoting the lower. With this form for ΔE , Eqs. (1) and (3) read

$$p(\sigma_g) = \frac{1}{1 + e^{-\sigma_g \alpha(V - V_b)}} \quad (6)$$

and

$$p_o(V) = \frac{1}{1 + e^{-\alpha(V - V_b)}}. \quad (7)$$

This function $p_o(V)$ describes the data in Fig. 3. The constant α is determined from a fit to the data, or is estimated as

$$\alpha = 4 \left. \frac{dp_o}{dV} \right|_{V=V_b}. \quad (8)$$

Because α has a physical interpretation in terms of a gating charge

$$z = \alpha R/F/k_B \quad (9)$$

(with R the universal gas constant, F Faraday's constant, k_B Boltzmann's constant, and α in units of $k_B T$), α may and may not depend on the branch we describe. It is natural to assume that the gating charges are the same on both branches, while the mechanical forces that these charges pull against when opening and closing the gate may change between branches as result of a conformational change of the protein. Figure 3 shows that it is not a bad approximation to assume that α is the same for both branches. Thus, we assume this because it leaves us with the simplest model. Obviously, the data could be fitted better if we assumed different α -values for the two branches, since it gives us an extra fitting parameter. However, we cannot conclude whether such an improvement is statistically significant, nor whether a difference in α -values is, for lack of reliable error bars associated with our data. If better data were somehow produced, and significantly different α -values were found, that would open up a whole new and more complex discussion of how to interpret physically the difference between the branches. Here, we only establish a platform from which this more complex discussion is better conducted.

3.2. The whole hysteresis cycle

We have described each branch of the hysteresis cycle separately, so far, though using the same explanation. We proceed to combine the separate explanations in a single one. The first step in doing this consists in noting that what is referred to as the open (closed) state on one branch, seems physically to be the same open (closed) state of the gate on the other branch as well. This we conclude for the open state from the fact that its conductance is the same, irrespective of which branch the system is on. There could be several closed states, however. Only one is discernible, though, a state that is entered (exited) directly from (to) the one open state. So we assume that there is only one closed state as well.

As for dynamics, throughout this paper we assume that all transitions between open and closed states of gates, as well as changes in "gate tension," binary or continuous, are thermally driven stochastic processes that conform to the standard Markov-description. It should be noted that memory effects are modeled naturally with non-Markovian models [12–17]. Doing that would sacrifice the kinetic description that is normally used, however. As shown here, that is not necessary.

3.2.1. Hysteresis: The mechanism

The two branches differ w.r.t. V_b , so on one branch we must pull harder on the gate — by applying a larger membrane potential V — than we must on the other branch, in order to achieve the same probability for the gate being open. Clearly, the hypothetical spring that the gate pulls against when opening, has two states, a stiffer and a softer. So in addition to σ_g , the system must have another binary degree of freedom that takes different values on the two different branches of p_o 's hysteresis cycle. When sweeping the membrane potential up and down, this additional degree of freedom changes its binary value near the extremes of the potential's values, thus causing a cyclic change of states.

A simple physical explanation of this additional degree of freedom could be that the protein (the hypothetical spring, *e.g.*) has two different conformational states, $\sigma_c = \pm 1$, with different effects on the gating process, hence dubbed states of “gate tension.” Transitions between these states of gate tension depend on the state of the gate, and *vice versa*; see Figs. 4 and 5.

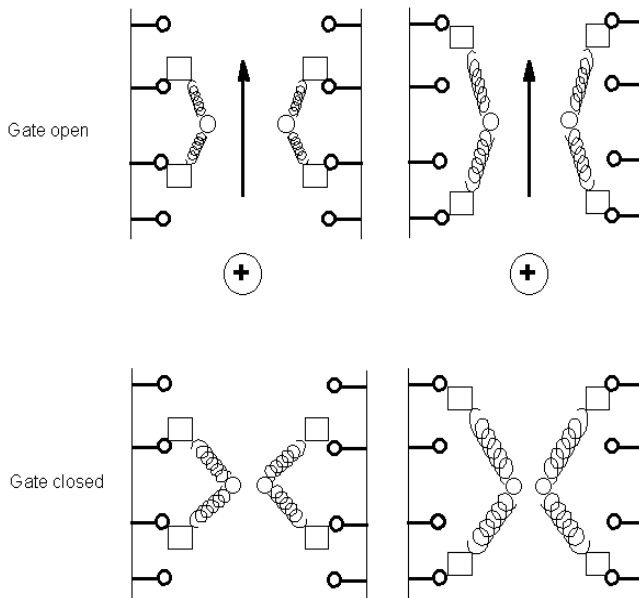


Fig. 4. Configurational changes of ion channel reflected in the pattern it opens and closes with as function of history. The traces shown were recorded from the red cell non-selective voltage activated cation (NSVDC) channel, clamped at +70 mV. When the command potential was increased step-wise from negative to positive values, the upper trace was obtained at +70 mV. When the command potential was decreased again, after full activation at +100 mV, the lower trace was obtained. Due to the heavy filtering (cut-off frequency 1 Hz) fast events are underrepresented.

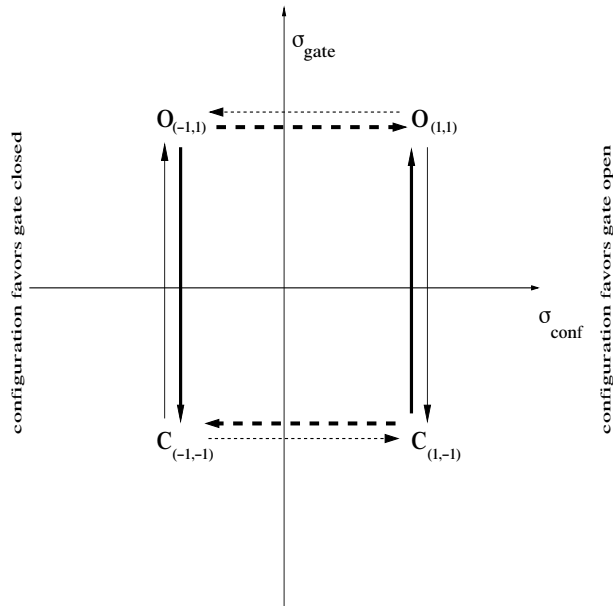


Fig. 5. The four states of the 2×2 -model: The upper two states have an open gate, the lower two, closed. The two states to the right favor open gate, the two to the left, closed. Transitions between open and closed gate (vertical transitions) are fast, while transitions between states favoring open/closed gates are slow, so slow that effectively only the time-averaged state of the gate — parametrized, *e.g.*, by its probability of being open — affects the slow dynamics.

One appealing consequence of this scenario is that Newton's third law explains the hysteresis observed: If the conformational state of the protein dubbed "gate tension" affects the state of the gate, then the state of the gate will exert an opposite force on this conformational state of the protein. For example, as follows: If the part of the protein that makes up the gate, is attached elastically to the rest, then when we pull at the gate with V , the gate pulls this rest in the same direction. If the protein has two different conformational states, it can yield to this pull, *i.e.*, change to a state of lower energy for the given state of the gate. The protein yields only unwillingly, we see, since two well-separated branches of $p_o(V)$ are observed. That is, the protein has a large energy barrier towards this change. *So, though driven by thermal excitation, the change only occurs if the pull is persistent, as it is at membrane potential values that force the gate to be either open all the time or closed all the time.*

Thus, when the system is on the lower branch, a closed gate is favored, and V must be chosen so large that the gate is open with overwhelming probability for a long time before the protein yields to the pull of the open

gate and makes a transition to a conformation that is energetically lower in the situation where the gate is open. Once it is there, however, an open gate is favored energetically also if we lower V again, *i.e.*, we are on the upper branch of $p_o(V)$.

So now V must be chosen so low that the gate is almost always closed, and kept there for a long time before the protein yields again, either to the pull of the closed gate, or, if there is no such thing, to its own internal restoring forces. When yielding in this manner, it changes its conformation of gate tension back to the one favoring a closed gate.

Thus we have hysteresis, a memory effect: The system's state reflects the system's history. Note that the hysteresis loop is looped in the counter-clockwise direction when we sweep V up and down sufficiently slowly and with sufficient amplitude. This direction is not ours to choose: it is forced upon us by the system's intrinsic dynamics, in response to our sweeping the voltage slowly up and down. Thus we already have a distinct consequence of our modeling: The direction of the hysteresis loop is counter clock-wise, as a simple consequence of Newton's third law; specifically, the protein yielding to the reaction force from its own pull or push at the gate.

3.2.2. Hysteresis: Energetics

We now model the system's intrinsic dynamics in the simplest possible mathematical manner.

The two conformational states of different gate tensions are labeled with the binary variable σ_c that takes the two values ± 1 , $+1$ referring to the upper branch, with half-way potential $V_b = V_+ = 54$ mV, and -1 referring to the lower branch, with half-way potential $V_b = V_- = 76$ mV; see Figs. 3 and 5.

Again, we associate an internal energy $E(\sigma_g, \sigma_c)$ with each of the now *four* states of the system. The most general function of the four values that (σ_g, σ_c) can take, can be written

$$E(\sigma_g, \sigma_c) = E_0 + \frac{1}{2}\Delta E_g \sigma_g + \frac{1}{2}\Delta E_c \sigma_c + \frac{1}{2}\Delta E_i \sigma_g \sigma_c. \quad (10)$$

For a given value of σ_c , this energy is the function $E(\sigma_g)$ of the previous subsection. In particular,

$$E(+1, \sigma_c) - E(-1, \sigma_c) = -\alpha(V - V_{\sigma_c}). \quad (11)$$

Here the left-hand-side can be calculated from Eq. (10),

$$E(+1, \sigma_c) - E(-1, \sigma_c) = \Delta E_g + \Delta E_i \sigma_c, \quad (12)$$

while V_{σ_c} 's dependence on σ_c can be written explicitly as

$$V_{\sigma_c} = \bar{V} - \Delta V \sigma_c, \quad (13)$$

where we have introduced

$$\bar{V} = \frac{1}{2}(V_+ + V_-) = 65 \text{ mV}, \tag{14}$$

$$\Delta V = \frac{1}{2}(V_- - V_+) = 11 \text{ mV}. \tag{15}$$

The numerical values given here follow from the fits in Fig. 3. Using all this in Eq. (11), we conclude that

$$\Delta E_g = -\alpha (V - \bar{V}), \tag{16}$$

$$\Delta E_i = -\alpha \Delta V. \tag{17}$$

Thus the internal energy $E(\sigma_g, \sigma_c)$ is a known function, determined from the fit shown in Fig. 3, except for the parameter ΔE_c which we shall return to, below

$$E(\sigma_g, \sigma_c) = E_0 - \frac{1}{2}\alpha (V - \bar{V}) \sigma_g + \frac{1}{2}\Delta E_c \sigma_c - \frac{1}{2}\alpha \Delta V \sigma_g \sigma_c. \tag{18}$$

Here E_0 is an arbitrary additive constant, and irrelevant in the sense that it disappears from all expressions in Boltzmann statistics, so we may as well set it equal to zero.

The last term in the internal energy depends on the *product* of σ_g and σ_c . It is an *interaction energy*. Since $\Delta V > 0$, this interaction favors that σ_g and σ_c have the same value. That reduces the internal energy, hence is favored by higher Boltzmann probability. This interaction term is the embodiment of Newton’s third law as referred to above: The force that the one degree of freedom exerts on the other, is the same as the force that the other degree of freedom exerts on the first.

3.2.3. Hysteresis: Probabilities

The probability that the gate is open/closed with the protein in the state favoring/discouraging this, is

$$p(\sigma_g, \sigma_c) = \mathcal{N} e^{-E(\sigma_g, \sigma_c)}, \tag{19}$$

where \mathcal{N} is a normalization factor defined as

$$\mathcal{N}^{-1} \equiv \sum_{\sigma_g=\pm 1} \sum_{\sigma_c=\pm 1} e^{-E(\sigma_g, \sigma_c)} \tag{20}$$

to make the total probability sum to one. The probability distribution $p(\sigma_g, \sigma_c)$ relates to the previous subsection’s *conditional* probabilities through the relation

$$p(\sigma_g, \sigma_c) = p(\sigma_g|\sigma_c) p(\sigma_c), \tag{21}$$

where $p(\sigma_g|\sigma_c)$ is the probability distribution for σ_g , given the value of σ_c . This is the probabilities considered in the previous subsection: the probability for the value of σ_g on a given branch of the hysteresis curve.

Summing over σ_g on both sides in Eq. (21) gives the probability that the protein is in a given conformation of gate tension

$$p(\sigma_c) = \sum_{\sigma_g=\pm 1} p(\sigma_g, \sigma_c). \quad (22)$$

Which conformation is favored for a given membrane potential V is most easily seen from the ratio

$$\frac{p(\sigma_c = +1)}{p(\sigma_c = -1)} = e^{-\Delta E_c} \frac{\cosh(\frac{\alpha}{2}(V - V_+))}{\cosh(\frac{\alpha}{2}(V - V_-))}. \quad (23)$$

In principle, ΔE_c may depend on the value V of the membrane potential. In practice, it is known not to, at least in a good first approximation. We assume this, as it keeps the modeling simpler, but keep in mind that we can reevaluate this assumption should the simplest modeling be insufficient. Thus, for here V is sensed only by the gate, by means of the charge that the gate carries for this purpose. But in principle a channel may feel the membrane potential V directly, via the stress that V builds in the membrane. This would constitute a mechanical contribution to ΔE_c , in addition to the one we already model, the electrical one felt via the gate.

ΔE_c can be measured at any value of V at which the protein is in thermal equilibrium w.r.t. its two conformational states of gate tension within the duration of the measurement. If such a value of V exists, one can measure the ratio between the time spent by the protein in each of its two conformations of gate tension, and identify that ratio with the ratio of Boltzmann probabilities in Eq. (23). Since α , V_+ , and V_- all are known from the fits in Fig. 3, ΔE_c can be then calculated from Eq. (23). If several such values of V exist, one has an experimental test of whether ΔE_c is independent of V , as assumed here.

The Boltzmann probabilities in Eq. (23) are not easily realized by the system, however. It will not equilibrate thermally between the protein's two states. This follows from the fact that we observe hysteresis: Hysteresis is a "memory effect", the system is confined to a region of its phase space, *i.e.*, it "remembers" which region it is in. This is the logical opposite of thermal equilibrium: The defining signature of thermal equilibrium is that the system explores its phase space fully, visiting all states with relative dwell times equal to their Boltzmann probabilities. Hysteresis is observed when a large energy barrier (large in units of $k_B T$) prevents the system from visiting parts of its phase space within the duration of our observation time, unless a change in an external parameter, in our case the membrane potential V ,

helps it over the barrier by pulling it in that direction. The barrier then prevents the system from going back, unless a change of sign in the external parameter helps it back.

In our case, the barrier separates $\sigma_c = +1$ from $\sigma_c = -1$, and only large/small values of V will allow σ_c to change. When such changes occur near the extremes of the hysteresis cycle, they may well be irreversible in the sense that the system passes from one branch to another, but not back again, because the barrier towards the forward change is small, while the barrier towards the backwards change is too large to be crossed thermally within the observation time. We return to this issue below.

At intermediate values of V , the system is stuck with the value that σ_c has, *i.e.*, stuck on a specific branch of the hysteresis cycle. So the hysteresis observed in Fig. 3 reveals that there is a large energy barrier separating the two states of the protein, a barrier preventing thermal equilibrium during our time of measurement. Boltzmann probabilities are consequently not realized, and ΔE_c is, therefore, not accessible in experiments based on equilibrium considerations.

3.2.4. Hysteresis narrows down the value for ΔE_c

For $V - V_- \gg \alpha^{-1}$, *i.e.*, at a high positive membrane potential, near the end of the hysteresis loop, Eq. (23) reads

$$\frac{p(\sigma_c = +1)}{p(\sigma_c = -1)} \approx e^{-\Delta E_c + \alpha \Delta V} . \tag{24}$$

Similarly, for $-(V - V_+) \gg \alpha^{-1}$, *i.e.*, at a low (negative) membrane potential, near the other end of the hysteresis, Eq. (23) reads

$$\frac{p(\sigma_c = +1)}{p(\sigma_c = -1)} \approx e^{-\Delta E_c - \alpha \Delta V} . \tag{25}$$

From the fact that hysteresis is observed, it follows that $p(\sigma_c = +1)/p(\sigma_c = -1) \gg 1$, where the potential is high, and $p(\sigma_c = +1)/p(\sigma_c = -1) \ll 1$, where the potential is low. Thus we must have $-\Delta E_c + \alpha \Delta V \gg 0$ and $-\Delta E_c - \alpha \Delta V \ll 0$, which combines to

$$-\alpha \Delta V \ll \Delta E_c \ll \alpha \Delta V . \tag{26}$$

From the fits in Fig. 3 we have $\alpha \Delta V = 1.4$, so Eq. (26) means $|\Delta E_c| \ll 1.4$.

3.2.5. Bottom line on 2×2 model

We conclude that the “ 2×2 ” model introduced here describes the hysteresis observed in the open-probability $p_o(V)$, including the direction of the

cycle. The only physics invoked is Boltzmann statistics, while the rest of the model is pure and minimalist phenomenology. Boltzmann statistics depends on the system having an internal energy. The only such energy possible for our minimalist model has Newton's third law as consequence for the interaction between the model's two degrees of freedom, and leaves us with only one parameter, ΔE_c , yet to be determined, its value already narrowed down to $|\Delta E_c| \ll 2.2$ when measured in units of $k_B T$.

4. Reaction pathway model: $2 \times \mathcal{R}$

4.1. The potential $W(x)$

In order to discuss the conformational change of gate tension quantitatively, we introduce a parametrization of the *reaction pathway* for this change. As above, we try with the simplest possible model. In this spirit, we use only a single real parameter, x , to describe the reaction pathway, and a corresponding potential $W(x)$ to describe the protein's internal energy as function of x . Thus σ_c is replaced by x , with the values $x \approx \pm 1$ corresponding to the states $\sigma_c = \pm 1$. In the system's internal energy, $\frac{1}{2}\Delta E_c \sigma_c$ is replaced by $W(x)$, where $W(x)$ has local minima at $x = \pm 1$ with values $W(\pm 1) = \pm \frac{1}{2}\Delta E_c$, and a barrier separating these two minima; see Fig. 6.

The simplest function $W(x)$ with these properties, three extrema, is a fourth-degree polynomial. Any real-valued fourth-degree polynomial is fully specified by five real parameters, *e.g.*, $(w_n, n = 0, \dots, 4)$ in $W(x) = \sum_{n=0}^4 w_n x^n$. The four demands, $W(\pm 1) = \pm \frac{1}{2}\Delta E_c$ and $W'(\pm 1) = 0$, determine four of these parameters. We reparametrize the polynomial so the last parameter is the value of the reaction coordinate x at which the local maximum, the top of the barrier between the minima, is located. We call it x_{\max} and have

$$W(x) = \Delta E_c \left(\frac{1}{4}x(3-x^2) + \frac{3}{16x_{\max}}(1-x^2)^2 \right). \quad (27)$$

The barrier maximum $E_{\max} = W(x_{\max})$ takes any value between $\frac{1}{2}|\Delta E_c|$ and ∞ for $-1 < x_{\max} < 1$. Thus qualitatively different barriers can be explored with this simplest form for $W(x)$, once we have redefined the interaction term. This can be done in as many ways as $x \neq \pm 1$ can affect the open-probability. Being clueless about this, we resort to Occam's Razor and replace $\frac{1}{2}\Delta E_i \sigma_g \sigma_c$ with the simplest possible form, $\frac{1}{2}\Delta E_i \sigma_g x$. Then

$$E(\sigma_g, x) = E_0 + \frac{1}{2}\Delta E_g \sigma_g + W(x) + \frac{1}{2}\Delta E_i \sigma_g x. \quad (28)$$

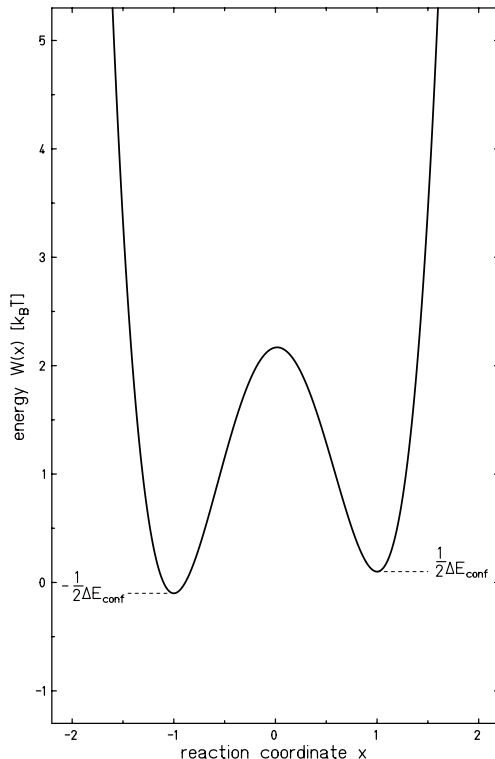


Fig. 6. Potential $W(x)$. The specific potential shown is that given in Eq. (27), but our considerations are valid for all potentials with the same qualitative form.

4.2. The effective potential $W_{\text{eff}}(x)$

Since the gate's thermally driven changes between its open and closed state take place much faster than the protein's changes of gate tension, the latter, parametrized by x , take place in the effective potential $W_{\text{eff}}(x; V)$ that results from summing over both states of the gate

$$\begin{aligned}
 e^{-W_{\text{eff}}(x; V)} &= p(x) \\
 &= \sum_{\sigma_g = \pm 1} p(\sigma_g, x) \propto \sum_{\sigma_g = \pm 1} e^{-E(\sigma_g, x)} \\
 &= e^{-E_0 - W(x)} 2 \cosh\left(\frac{1}{2} \Delta E_g(V) + \frac{1}{2} \Delta E_i x\right). \quad (29)
 \end{aligned}$$

Thus, up to an additive constant, the x -dependence of W_{eff} is

$$\begin{aligned}
 W_{\text{eff}}(x; V) \\
 &= W(x) - \log\left(\cosh\left(\frac{1}{2} \Delta E_g + \frac{1}{2} \Delta E_i x\right)\right)
 \end{aligned}$$

$$\begin{aligned}
&= W(x) - \log \left(\cosh \left(\frac{1}{2} \alpha (V - \bar{V} + \Delta V x) \right) \right) \\
&= W(x) - \log \left(\cosh (0.07(V - 65) + 0.7 x) \right), \tag{30}
\end{aligned}$$

where the last, numerical expression assumes that V is measured in millivolts.

$W_{\text{eff}}(x; V)$ relates to $W(x)$ as follows:

- (i) $W_{\text{eff}}(0; \bar{V}) = W(0)$. This is just a way to fix their relative value. Any constant w.r.t. x can be added to either potential without changing the physics they describe. With $W_{\text{eff}}(0; 0) = W(0)$, however, we have chosen to add the same constant to both potentials hereafter, should we choose to add any.
- (ii) The values of the function \cosh are larger than one, except for vanishing argument, where it is equal to one. So $-\log(\cosh(\dots)) \leq 0$, *i.e.*, $W_{\text{eff}}(x) \leq W(x)$; see Fig. 7.
- (iii) Since $W(x)$ ensures that $|x|$ rarely exceeds 1 by much, for $V = \bar{V}$ we can approximate $-\log(\cosh(0.7 x)) = -\log(1 + 0.25x^2 + 0.01x^4 + \dots) \approx -0.25x^2$. Thus the barrier separating the two minima of $W_{\text{eff}}(x; V)$ is more narrow near $W_{\text{eff}}(x; V)$'s maximum than the similar barrier in $W(x)$ is; see Fig. 7. The local maximum value of $W_{\text{eff}}(x; \bar{V})$, acquired near $x = 0$, is essentially unchanged because we have $W_{\text{eff}}(0; \bar{V}) = W(0)$; see Fig. 7. The barrier's height relatively to the two minima changes, however.
- (iv) When the argument of the function \cosh is numerically large, it is well approximated by $\cosh(x) \simeq \frac{1}{2} \exp(|x|)$. This approximation corresponds mathematically to inclusion of only the largest of the two terms in the sum over σ_g in Eq. (29). Physically, it corresponds to assuming that the gate remains open all the time, or it remains closed, depending on which is favored. This approximation applies for values of V near the extremes of the hysteresis loop.
- (v) Thus, for $V - \bar{V}$ large, *e.g.*, larger than $3\Delta V$

$$\begin{aligned}
W_{\text{eff}}(x; V) &\simeq W(x) - \frac{1}{2} \alpha (V - \bar{V} + \Delta V x) + \log 2 \\
&= W(x) + \frac{1}{2} \Delta E_g(V) + \frac{1}{2} \Delta E_i x + \log 2, \tag{31}
\end{aligned}$$

and we note that the explicitly written terms favor $x = +1$ over $x = -1$ with an energy difference of $\alpha \Delta V = |\Delta E_i|$, as they should by construction. However, we also note that the energy barrier at $x \approx 0$ between the states of different gate tensions, $x = \pm 1$, has been lowered by an amount $\frac{1}{2} \alpha (V - \bar{V}) = \frac{1}{2} |\Delta E_g(V)|$; see Fig. 7.

(vi) Identical reasoning for $V - \bar{V}$ large negative gives

$$W_{\text{eff}}(x; V) \simeq W(x) + \frac{1}{2}\alpha (V - \bar{V} + \Delta V x) + \log 2, \quad (32)$$

and the barrier at $x \approx 0$ has again been lowered by $\frac{1}{2}\alpha|V - \bar{V}| = \frac{1}{2}|\Delta E_g(V)|$, while for this range of V -values $x = -1$ is favored over $x = +1$, with the same energy difference $\alpha\Delta V = |\Delta E_i|$; see Fig. 7.

We do not explore the consequences of the specific forms of $W(x)$ and $W_{\text{eff}}(x; V)$, but simplify further by approximating the thermally driven barrier crossing with the simplest single-barrier scenario. By doing that, we capture the essential behavior of the system for a much larger set of possible potentials.

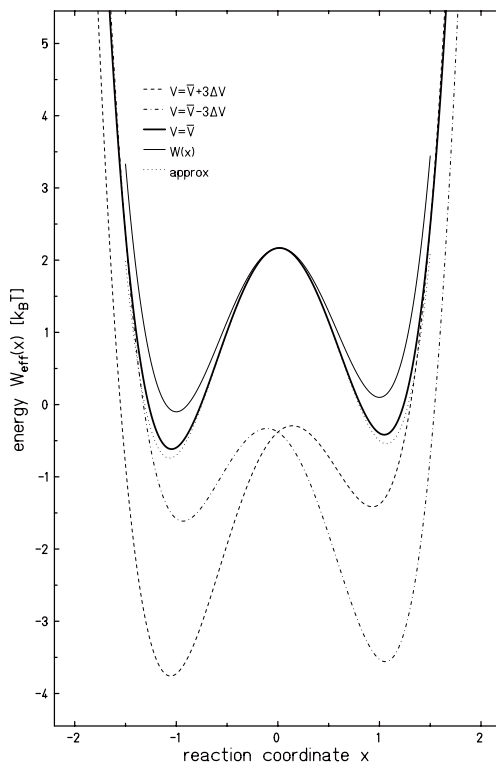


Fig. 7. The effective potential for changes of gate tension, $W_{\text{eff}}(x; V)$, for $V = \bar{V}$ (thick line), $V = \bar{V} + 3\Delta V$ (dashed), and $V = \bar{V} - 3\Delta V$ (dash-dotted). Also shown: $W(x)$ (thin line) and approximation for $W_{\text{eff}}(x; \bar{V})$ valid for x not large (dotted line).

4.3. Switching branches by thermal barrier crossing

The rates of escape from one branch of $p_o(V)$ to another follow the Van't Hoff–Arrhenius law, see [18]

$$k_{+-}(V) = \nu_{+-} e^{-(W_{\text{eff}}(x_{\text{max}}, V) - W_{\text{eff}}(1, V))}, \quad (33)$$

$$k_{-+}(V) = \nu_{-+} e^{-(W_{\text{eff}}(x_{\text{max}}, V) - W_{\text{eff}}(-1, V))}. \quad (34)$$

Note that the parameter $\beta = 1/k_{\text{B}}T$ that usually occurs in front of the activation energies $W_{\text{eff}}(x_{\text{max}}, V) - W_{\text{eff}}(\pm 1, V)$ in this kind of expressions, equals one here, because we have chosen to give all energies in units of $k_{\text{B}}T$. We have approximated the two values of x that minimize $W_{\text{eff}}(x; V)$ with $x = \pm 1$. These x -values minimize $W(x)$ by design, and for this reason they are also good approximations to the x -values minimizing W_{eff} . We have also approximated the x -value maximizing W_{eff} , the “transition state,” with the one maximizing W , for the same good reason. Soon, we shall also approximate x_{max} with 0, where convenient. The Van't Hoff–Arrhenius law is the result of an approximation itself, and we shall only discuss its leading-order terms, the exponential expressions above.

The sub-leading prefactors ν_{+-} and ν_{-+} are given in terms of $\partial^2 W_{\text{eff}}(x; V)/\partial x^2$ at the x -values extremizing W_{eff} in Kramers reaction rate theory [18]. These second derivatives depend on $\partial^2 W(x)/\partial x^2$, *i.e.*, on details regarding the form of $W(x)$ that we have no access to via the data shown in Fig. 3. The expression for $W(x)$ given in Eq. (27) is just the simplest one we could write down. So we have reached the limit for how much information we can extract from the data in Fig. 3. Consequently, the approximations done for x 's extremum values fully satisfy our thus limited purpose. The three x -values ± 1 and $x_{\text{max}} \approx 0$ represent the two favored conformations of gate tension and the transition state connecting them.

Equations (33) and (34) are generally valid expressions, limited only to the range of validity of the Van't Hoff–Arrhenius law. In the situations, where branch switching actually occur, *i.e.*, near the two extremes of the hysteresis cycle, we can use the approximate expressions in Eq. (31) to find

$$k_{+-} = \nu_{+-} e^{-(W(0) - W(1) + \frac{1}{2}\alpha\Delta V)}, \quad (35)$$

$$k_{-+} = \nu_{-+} e^{-(W(0) - W(-1) - \frac{1}{2}\alpha\Delta V)} \quad (36)$$

for $V - \bar{V}$ large, *e.g.*, larger than $3\Delta V$. Similarly, Eq. (32) gives

$$k_{+-} = \nu_{+-} e^{-(W(0) - W(1) - \frac{1}{2}\alpha\Delta V)}, \quad (37)$$

$$k_{-+} = \nu_{-+} e^{-(W(0) - W(-1) + \frac{1}{2}\alpha\Delta V)} \quad (38)$$

for $V - \bar{V}$ large negative, *e.g.*, less than $-3\Delta V$.

The ratio between rates of opposite directions gives the probability that the system is on a given branch, when the rates are sufficiently large to ensure transitions between branches. This is the case near the two extremes of the hysteresis cycle, where transition in at least one direction occurs. For $V - \bar{V}$ large, the ratio of favorable to unfavorable transition rate is

$$\begin{aligned}
 k_{-+}/k_{+-} &= \nu_{-+}/\nu_{+-}e^{-\Delta E_c + \alpha\Delta V} \\
 &= \nu_{-+}/\nu_{+-}e^{-\Delta E_c + 1.4} \\
 &\approx 4e^{-\Delta E_c} \\
 &\approx 4 \text{ for } \nu_{-+}/\nu_{+-} \approx 1,
 \end{aligned}
 \tag{39}$$

where Eq. (26) has been used. This result can also be obtained directly from Eq. (23) using detailed balance. The present derivation makes clearer, however, what approximations are involved. Similarly, for $V - \bar{V}$ large negative, the ratio of favorable to unfavorable transition rate is

$$\begin{aligned}
 k_{+-}/k_{-+} &= \nu_{+-}/\nu_{-+}e^{\Delta E_c + \alpha\Delta V} \\
 &= \nu_{+-}/\nu_{-+}e^{\Delta E_c + 1.4} \\
 &\approx 4e^{\Delta E_c} \\
 &\approx 4 \text{ for } \nu_{+-}/\nu_{-+} \approx 1.
 \end{aligned}
 \tag{40}$$

4.4. Looping the loop

We have by now established the necessary formulas to explain the physics behind the hysteresis loop in semi-quantitative terms. We can start the explanation anywhere on the loop, but assume $V - \bar{V} \ll -\Delta V$ for a start, so that V has one of the lowest values shown in Fig. 3. That strongly favors $\sigma_g = -1$, so the system spends most of its time in the lower half of the kinetic diagram in Fig. 5. Figure 7 shows that this results in a low activation energy for the transition $(\sigma_c = +1) \rightarrow (\sigma_c = -1)$ and a high activation energy for the opposite transition. So if $\sigma_c = -1$ initially, it keeps that value with overwhelming probability because the barrier towards change is very high. If, on the other hand, $\sigma_c = +1$ initially, the probability per unit time that it changes value to -1 is high, because the barrier towards change is low. Once changed to -1 , this value is kept, because the barrier towards change back to $+1$ is very high, as already mentioned. This equilibrium, strongly biased towards $\sigma_c = -1$, is symbolized with the two dashed arrows connecting $C_{(-1,-1)}$ and $C_{(1,-1)}$ in Fig. 5.

If we now increase V by a few ΔV , σ_c remains equal to -1 because the barrier towards change remains high. It decreases though, because the larger membrane potential biases the gate towards being open, a bias that

is counteracted by the bias on the gate from the state of gate tension favoring a closed gate. This equilibrium, strongly biased towards $\sigma_g = -1$, is symbolized with the two arrows connecting $C_{(-1,-1)}$ and $O_{(-1,1)}$ in Fig. 5.

When the membrane potential is increased more, its bias towards an open gate gradually wins over the bias on the gate from the conformation favoring a closed gate, and the gate is more frequently open. This means that the equilibrium between $C_{(-1,-1)}$ and $O_{(-1,1)}$ in Fig. 5 is shifted increasingly towards $O_{(-1,1)}$. This is the situation on the lower branch in Fig. 3 for $V = 50\text{--}90\text{ mV}$.

When the membrane potential is increased so much that it forces the gate to be predominantly open, against the bias caused by the gate tension, $O_{(-1,1)}$ is strongly favored over $C_{(-1,-1)}$. This describes the situation on the lower branch at the right extreme of the hysteresis loop in Fig. 3. This is a meta-stable state because of Newton's third law: The protein pulls at the gate to close, but the opposite equal force from the gate on the protein pulls at its conformation of gate tension, favoring a transition to $O_{(1,1)}$. The energetics of this is illustrated in Fig. 7, and the equilibrium, strongly biased towards $O_{(1,1)}$, is represented by the two dashed arrows connecting $O_{(-1,1)}$ and $O_{(1,1)}$ in Fig. 5.

$O_{(1,1)}$ is a state on the upper branch in Fig. 3. With the system there, an open gate is favored over a closed one by the state of the gate tension. This is symbolized by the two arrows connecting $O_{(1,1)}$ and $C_{(1,-1)}$. The large membrane potential that brought us to the state $O_{(1,1)}$ also favors an open gate. But if we lower the membrane potential now, the gate remains predominantly open due to bias from the gate tension, until V is well below \bar{V} and overcomes this bias. Then $C_{(1,-1)}$ is favored over $O_{(1,1)}$. This is the situation on the left part of the upper branch in Fig. 3.

With even lower values for V the system is strongly biased towards $C_{(1,-1)}$. This is a meta-stable state, due to Newton's third law again: The protein pulls at the gate to open, but the opposite equal force from the gate on the protein pulls at its conformation, favoring a transition to $C_{(-1,-1)}$, the transition with which we started this subsection. We have come full circle on the hysteresis loop.

So far we have treated hysteresis as if we could sweep out the loop at a pace of our own choosing, except near its extremes, where we must wait long enough for branch switching to occur. This *is* a correct description, as long as we are not too slow. After all, we have repeatedly invoked Boltzmann statistics, and given sufficient time, it crosses any barrier. Thus the area of the hysteresis loop depends on how fast we sweep through it: The slower/faster we sweep, the smaller/larger its area, and the shorter/longer is the interval of voltage in which two branches exist. At any given speed, one can ask how well defined are the extremes of the recorded loop? This is the subject of the next section.

5. Discussion

5.1. Experiments?

Changes in σ_g and σ_c take place at very different rates. Suppose, however, that we could measure for so long that indeed many of the slowest transitions have taken place. Then we could estimate from the data the equilibrium probabilities for given V that the system is in any one of its *four* states $(\sigma_g, \sigma_c) = (\pm 1, \pm 1)$, and ΔE_{conf} could be found from the relative amount of time that σ_c spends in either state.

To do this measurement, in either end of the hysteresis loop one must record time series for σ_g , and then within these series find subseries characterized by a different value for σ_c . The signature characteristic of such subseries is a different value for p_o , as well as different rates of change between open and closed. Then ΔE_{conf} can be found from the relative amount of time σ_c spends in either state.

If such subseries really *are* found, a reinterpretation of experimental series is necessary in order to find more correct values for the hysteresis branches. As they stand, data for each branch are then contaminated by an admixture of data belonging to the other branch. That is what such subseries are, data from another branch. The average duration of either such subseries, on the other hand, gives the barrier height for transitions to the branch corresponding to the other type of subseries in a simple Kramers scenario.

These experiments may not be feasible because the slowest event, crossing of the tallest barrier in W_{eff} , is too rare. In this case, one may instead try to measure the lowest of the two barriers in W_{eff} , by measuring the waiting time to barrier crossing following a rapid change of membrane potential V from one of its extreme values — held for long enough to ensure that the protein's configuration has relaxed — to an opposite near-extreme value. This near-extreme value should be sufficiently extreme for transitions to occur at a measurable rate, yet far enough from the extreme for p_o to differ measurably, and quickly so, between the two configurational states. This experiment is only feasible if at both ends of the hysteresis cycle such values exist for the membrane potential. If they do exist, and ΔE_c is independent of V , as assumed above, then the ratio between the two barrier transition rates that one can obtain in this manner, determine ΔE_c , when interpreted with Van't Hoff–Arrhenius law, as above.

5.2. Interpretations?

Hysteretic gating behavior of ion channels may well be an important physiological property. As demonstrated in the analysis presented here, the simplest standard kinetics of opening or closing is sufficient to cause strong

hysteresis in a channel. All it takes, is an ability in the protein to yield unwillingly to a sustained force from the gate. Thus hysteresis is likely to be realizable in essentially any complex ion channel under suitable experimental or physiological conditions. According to the broad definition of the phenomenon, any reproducible difference in paths of activation and deactivation may be categorized as hysteretic behavior. Strictly speaking, this will include all ion channels that exhibit inactivation or desensitization, and, therefore, arrive at a non-conducting state already during activation. Examples are the voltage-dependent Na-channel that initiates action potentials in excitable tissues (inactivation) and most neurotransmitter activated channels (desensitization).

Accordingly, Na-channel memory must be considered a fundamental property of the normal action potential: As can be implied from the conventional Na-channel kinetics (see [19]), the channel activates during upstroke, profoundly inactivates at the peak, and finally deactivates during the repolarization and afterhyperpolarization phases. A simple plot of the Na-channel conductance (or p_o) against the action potential cycle reveals profound hysteresis. Though consistent with the definition of hysteresis, these examples are obvious and perhaps trivial cases, and the concept of hysteresis will hardly add significantly to our understanding of the action potential *per se*.

More adaptive changes, occurring on a much slower time-scale and possibly superimposed on and influencing the normal channel gating, would be more interesting cases of hysteresis. Such slow internal changes in channel-gating may well contribute to synaptic as well as extrasynaptic plasticity phenomena that are normally attributed to activity-dependent biochemical changes in neurons. Instead, or as a supplement, we have activity-dependent biophysical changes in channels.

6. Conclusions

We have demonstrated that hysteretic behavior can be expected from a single molecule that has just 2×2 states and well-separated intrinsic time-scales for thermal transitions between pairs of these states. Hysteresis then occurs when we apply an external bias to the binary degree-of-freedom with the fast transition, and sweep this bias slowly as compared to that transition, but fast as compared to the system's slow transition [20–24]. Since it seems to be the rule, rather than the exception, that channels have multiple states, hysteresis may be a common phenomenon.

Effects of molecular memory have been previously discussed in other kinetic diagrams explaining fractal gating of biological channels [25–28]. The energy level analysis on those models was based on the assumption that the probability for a channel protein to switch states depends not only on

the present state, but also on how long the channel protein has already remained in that state. In fact, several studies had shown that the PDFs of the closed and open durations implied that the longer a channel protein remains in a state, the less the probability per second that it will exit that state [14, 17, 28]. These studies found that the typical relationship had a power law fractal scaling form where the probability per second to exit a state was proportional to t^d , where t is the time that the channel has been in a given state and $d > 1$ stands for the fractal dimension.

In a Markov gating process, the probability per unit of time to switch states depends only on the present state of the channel. Accordingly, channel data must satisfy so-called Smoluchowski–Chapman–Kolorogorov equation (SCKE). Analysis of potassium currents through channels of locust muscle membrane [14] demonstrated that deviations from the SCKE relationship were more than one order of magnitude higher than those for a test model based on a Markov process. These observations suggested that dynamical, time-dependent processes which cannot be described by Markov processes are, most likely, present in channel function and have initiated further studies of synthetically designed nanopores which can serve as models of biological channels [13, 29]. Altogether, further developments of existing models and new approaches are required to better describe the dynamical properties of channel proteins and to discriminate between information gained by Markov and non-Markov modeling of voltage-gated channels.

We thank Erik Hviid Larsen for reading the manuscript. E.G-N. thanks the *Danish Research Agency's Graduate School of Biophysics* for hospitality during her visit to the Niels Bohr Institute and August Krogh Institute in Copenhagen and the *European Science Foundation* via the Exploring Physics of Small Devices (EPSD) program.

REFERENCES

- [1] B. Hille, *Ionic Channels of Excitable Membranes*, Sinauer Associates Inc., Sunderland, Massachusetts, 2nd edition, 1992.
- [2] H. Duclohier *et al.*, *Biochim. Biophys. Acta* **1420**, 14 (1999).
- [3] L. Nowak, J.M. Wright, *Neuron* **8**, 181 (1992).
- [4] P.S. Pennefather, W. Zhou, T.E. DeCoursey, *J. Gen. Physiol.* **111**, 795 (1998).
- [5] W. Zhou *et al.*, *J. Gen. Physiol.* **111**, 781 (1998).
- [6] P. Christophersen, P. Bennekou, *Biochim. Biophys. Acta* **1065**, 103 (1991).
- [7] P. Christophersen, P. Bennekou, *Acta Physiol. Scand.* **143**, A30 (1991).

- [8] L. Kaestner, P. Christophersen, I. Bernhards, P. Bennekou, *Bioelectrochemistry* **52**, 117 (2000).
- [9] H. Xu *et al.*, *Nature* **418**, 181 (2002).
- [10] B.M. McCoy, T.T. Wu, *The Two-dimensional Ising Model*, Harvard University Press, Cambridge 1973.
- [11] A.L. Hodgkin, A.F. Huxley, *J. Physiol. (Lond.)* **117**, 500 (1952).
- [12] S. Mercik, K. Weron, Z. Siwy, *Phys. Rev.* **E60**, 7343 (1999).
- [13] Z. Siwy, A. Fuliński, *Phys. Rev. Lett.* **89**, 158101 (2002).
- [14] A. Fuliński *et al.*, *Phys. Rev.* **E58**, 919 (1998).
- [15] J. Timmer, S. Klein, *Phys. Rev.* **E55**, 3306 (1997).
- [16] A. Toib, V. Lyakov, S. Marom, *J. Neurosci.* **18**, 1893 (1998).
- [17] W.A. Varanda, L. Liebovitch, J. Figueiroa, R.A. Nogueira, *J. Theor. Biol.* **206**, 343 (2000).
- [18] P. Hänggi, P. Talkner, M. Borkovec, *Rev. Mod. Phys.* **62**, 251 (1990).
- [19] M.P.G. Korsgaard, P. Christophersen, P.K. Ahring, S.P. Olesen, *Pflgers Arch* **443**, 18 (2001).
- [20] J. Juraszek, B. Dybiec, E. Gudowska-Nowak, *Fluct. Noise. Lett.* **5**, L259 (2005).
- [21] M.A. Pustovoit, A.M. Berezhkovskii, S.M. Bezrukov, *J. Chem. Phys.* **125**, 194907 (2006); D. Petracchi *et al.*, *J. Stat. Phys.* **70**, 393 (1993).
- [22] T. Andersson, *Math. Biosci.* **226**, 16 (2010).
- [23] E. Gudowska-Nowak, H. Flyvbjerg, P. Bennekou, P. Christophersen, *AIP Conf. Proc.* **665**, 305 (2003).
- [24] E. Gudowska-Nowak, P. Christophersen, P. Bennekou, H. Flyvbjerg, *Biophys. J.* **84**, 488A (2003).
- [25] L.S. Liebovitch, *Biophys. J.* **52**, 979 (1987); L.S. Liebovitch, J. Fischbarg, J. Koniarek, *Math. Biosci.* **84**, 37 (1987).
- [26] S.B. Lowen, L.S. Liebovitch, J.A. White, *Phys. Rev.* **E59**, 5970 (1999).
- [27] S.J. Korn, R. Horn, *Biophys. J.* **54**, 871 (1988).
- [28] M.S.P. Sansom *et al.*, *Biophys. J.* **56**, 1229 (1989).
- [29] C. Tasserit *et al.*, *Phys. Rev. Lett.* **105**, 260602 (2010).